

MET Tyrosine Kinase Inhibition Enhances the Antitumor Efficacy of an HGF Antibody

Pamela J. Farrell¹, Jennifer Matuszkiewicz¹, Deepika Balakrishna¹, Shweta Pandya¹, Mark S. Hixon¹, Ruhi Kamran¹, Shaosong Chu², J. David Lawson³, Kengo Okada⁴, Akira Hori⁴, Akio Mizutani⁴, Hidehisa Iwata⁴, Ron de Jong¹, Barbara Hibner⁵, and Patrick Vincent¹



Abstract

Receptor tyrosine kinase therapies have proven to be efficacious in specific cancer patient populations; however, a significant limitation of tyrosine kinase inhibitor (TKI) treatment is the emergence of resistance mechanisms leading to a transient, partial, or complete lack of response. Combination therapies using agents with synergistic activity have potential to improve response and reduce acquired resistance. Chemoreagent or TKI treatment can lead to increased expression of hepatocyte growth factor (HGF) and/or MET, and this effect correlates with increased metastasis and poor prognosis. Despite MET's role in resistance and cancer biology, MET TKI monotherapy has yielded disappointing clinical responses. In this study, we describe the biological activity of a selective, oral MET TKI with slow off-rate and its synergistic antitumor effects when combined with an anti-HGF antibody. We evaluated the combined

action of simultaneously neutralizing HGF ligand and inhibiting MET kinase activity in two cancer xenograft models that exhibit autocrine HGF/MET activation. The combination therapy results in additive antitumor activity in KP4 pancreatic tumors and synergistic activity in U-87MG glioblastoma tumors. Pharmacodynamic characterization of biomarkers that correlate with combination synergy reveal that monotherapies induce an increase in the total MET protein, whereas combination therapy significantly reduces total MET protein levels and phosphorylation of 4E-BP1. These results hold promise that dual targeting of HGF and MET by combining extracellular ligand inhibitors with intracellular MET TKIs could be an effective intervention strategy for cancer patients who have acquired resistance that is dependent on total MET protein. *Mol Cancer Ther*; 16(7): 1269–78. ©2017 AACR.

Introduction

MET receptor tyrosine kinase (RTK) and its ligand hepatocyte growth factor (HGF) regulate biological processes involved in tumor initiation, progression, and metastasis, including cell proliferation, survival, migration, invasion, and angiogenesis (for recent reviews, see refs. 1–3). Upon stimulation by HGF, the MET receptor dimerizes, transphosphorylates, and recruits proteins that activate MAPK, STAT3, and PI3K/AKT pathways. Pathway activation is terminated when phosphorylated MET is internalized and degraded (4, 5). HGF/MET signaling evokes changes in gene transcription and protein stability setting up a complex

invasive growth program (6) that, if left unchecked, can result in unregulated cell proliferation, survival, and metastasis. MET and HGF alterations have been detected in gastric cancer, non-small cell lung cancer (NSCLC), hepatocellular carcinoma, colorectal cancer, renal cell cancer, breast cancer, ovarian cancer, and glioblastoma (2, 7). Somatic MET gain-of-function mutations, MET gene amplification, elevated MET, and elevated HGF are among the alterations reported (8). In addition, HGF and MET are implicated as resistance mechanisms for tyrosine kinase inhibitors (TKI) or chemotherapy in the treatment of NSCLC, pancreatic cancer, breast cancer, squamous cell carcinoma, and colon cancer (9–18). As a result of the strong biological connection to tumor initiation and progression, HGF and MET have been heavily pursued as strategies to treat cancer (19).

Numerous preclinical rodent studies have provided proof of concept for use of HGF and MET inhibitors in the treatment of cancers with activated HGF/MET signaling. Therapeutic approaches that have advanced to human trials include small-molecule MET TKIs, monoclonal antibodies to neutralize HGF, and antibodies targeting MET (19, 20). On the other hand, clinical results from HGF/MET monotherapies have been disappointing which may reflect targeting inappropriate cancers, insufficient pathway inhibition, and/or development of resistance mechanisms (21). To address these points, we designed Compound 1, a new durable MET TKI, tested it in combination with an HGF-neutralizing antibody, and investigated resistance mechanisms. Previous data have shown that dual inhibition of EGFR family members with a receptor antibody and TKI resulted in an

¹Department of Biological Sciences, Takeda California, San Diego, California.

²Department of Chemistry, Takeda California, San Diego, California. ³Department of Computational Sciences and Crystallography, Takeda California, San Diego, California. ⁴Pharmaceutical Research Division, Takeda Pharmaceutical Companies Ltd, Shonan, Japan. ⁵Oncology Biology, Takeda Boston, Cambridge, Massachusetts.

Note: Supplementary data for this article are available at Molecular Cancer Therapeutics Online (<http://mct.aacrjournals.org/>).

Current address for S. Pandya: Illumina, Inc., San Diego, CA 92122.

Corresponding Author: Pamela J. Farrell, Takeda California, 10410 Science Center Drive, San Diego, CA 92121. Phone: 858-335-8161; E-mail: pw2h@att.net

doi: 10.1158/1535-7163.MCT-16-0771

©2017 American Association for Cancer Research.

enhanced antitumor effect compared with single agents (22–26). Knowing an HGF-neutralizing antibody sensitizes MET-addicted tumors to MET-targeted agents (27), we hypothesized that dual inhibition of MET ligand and MET tyrosine kinase activity may also result in enhanced antitumor effect. Using the combination of two modalities that inhibit distinct targets in the same pathway represents an attractive therapeutic approach to treat cancer.

In this investigation, a unique and highly selective MET TKI (Compound 1) was designed and characterized. Compound 1's residence time on MET is much longer than other selective TKIs, and it potently inhibits biological activity of MET in human cancer cells *in vitro* and in xenograft models. Notably, combination treatment of Compound 1 with an HGF-neutralizing therapeutic antibody significantly improves the antitumor effect of each monotherapy, by a mechanism that involves reduction of the total MET protein. This combination approach has the potential to produce a sustained response in cancer patients with malignancies dependent on MET and/or for cancer patients who have developed a therapeutic resistance that is dependent on MET.

Materials and Methods

Reagents

Small-molecule MET TKI compounds were synthesized at Takeda California as described in WO2010/019899A1 (Compounds 1, 2, and 3), WO2007/132308A1 (PF04217903), and WO2006/021881A2 (crizotinib). Compounds 1, 2, and 3 correspond to examples 45, 3, and 13, respectively, in WO2010/019899A1. TAK-733 was synthesized at Takeda California as described in US8030317B2. Picilisib was from Selleckchem. TAK-701 (HuL2G7, Lot H701-001) was produced by Lonza Biologics. The L2G7 hybridoma is deposited with the American Type Culture Collection (ATCC). Antibodies for Western blotting were from Cell Signaling Technology.

Enzyme assessments

MET enzyme activity assays were performed as described in WO2010/019899A1 using a capillary electrophoresis with Caliper LifeSciences LabChip 3000 and fluorescence-based quantification of the phosphorylated peptide substrate 5-carboxyfluorescein-EAIYAAPFAKKK-CONH₂. IC₅₀ values were calculated by nonlinear least squares curve fitting of the standard IC₅₀ equation to background-corrected MET velocity versus compound concentration.

For determination of compound dissociation rate, an enzyme-inhibitor dilution assay was performed using the AlphaScreen method (Perkin Elmer). Briefly, MET enzyme (at 100-fold higher concentration than the final reaction condition) and each test compound (at 10-fold higher concentration than IC₅₀ value) were incubated together for 60 minutes at room temperature to form enzyme-inhibitor complex. This complex was diluted 1:100 into a reaction buffer containing 1 mmol/L ATP and 0.1 mg/mL biotinylated poly-Glu-Tyr (4:1), initiating the kinase reaction. Recovery of enzyme activity was monitored over time, and enzyme kinetic parameters were derived using slow binding inhibition equations (28).

Cells and culture

The MKN45 human gastric adenocarcinoma, EBC-1 human lung squamous cell carcinoma, and KP4 human pancreatic ductal carcinoma cell lines were obtained in 2007 from the Japanese

Collection of Research Bioresources Cell Bank. The SNU-5 gastric carcinoma and U-87MG malignant glioblastoma cell lines were obtained in 2006 and 2002, respectively, from ATCC. Cells were obtained directly from the indicated source, stored in liquid nitrogen, and cultured according to the supplier's recommendations for fewer than 4 months after resuscitation. Cell lines were confirmed authentic and mycoplasma negative by the supplier and/or by IDEXX BioResearch CellCheck and STAT-Myco assays.

Cellular assessments

Cells were seeded in 96-well microtiter plates at 4,000 to 10,000 cells per well and incubated with serial dilutions of compound for 48 or 72 hours. Cell viability was determined using the MTS assay or Cell Titer-Glo ATP assay (Promega). The compound concentration required to inhibit half of the maximal effect (IC₅₀) was determined from 11-point dose-response curves. Cellular selectivity assays were performed using stable BaF3 cell lines that were engineered to be dependent on the activity of a heterologous kinase for survival (Advanced Cellular Dynamics). For the mechanism-based assay, cells were seeded as indicated above and incubated for 2 hours with serial dilutions of compound. The level of phosphorylated MET versus total MET was determined using quantitative immune assays [BioSource International, Inc. (pY1230, pY1234, pY1235) or Meso Scale Diagnostics (pY1349)]. The durability of compound effect on suppression of phosphorylated MET was measured in MKN45 cells (50,000 cells per well), which were treated with 1 μmol/L compound for 2 hours prior to wash out. Cells were subsequently washed and incubated in growth media for 0, 1, 2, 4, 8, 12, 24, and 48 hours.

Tumor biomarkers and pharmacodynamics

Tumors were dissected and immediately snap-frozen at –80°C. Tumor tissue lysates were prepared in ice-cold cell extraction buffer (Thermo Fisher Scientific) supplemented with protease and phosphatase inhibitors (EMD Millipore) using a fast prep bead beater (Biospec Products, Inc.). After centrifugation, tumor lysates were diluted to equal protein concentration and analyzed for phosphorylated MET versus total MET using the immune assays described above or for other proteins using standard Western blot procedures. For pharmacokinetic (PK) analysis, plasma was collected via centrifugation of blood samples, and then stored at –80°C until compound content was analyzed using a research grade LC/MS/MS assay. PK parameters were determined with the WinNonlin software. Unbound (free) drug was estimated using species-specific percent protein binding, determined by equilibrium dialysis.

In vivo models and test article administration

All animal studies were conducted in accordance with Takeda Institutional Animal Care and Use Committee guidelines in a facility accredited by the American Association for Accreditation of Laboratory Animal Care. Female athymic nude mice (Hsd: Athymic Nude-Foxn^{nu}) were purchased from Harlan Laboratories for MKN45 xenografts and female athymic nude mice (BALB/cA/Jcl-nu/nu) from Japan Clea for KP4 xenografts. Mice were housed in a barrier facility with 12-hour light/dark cycles and provided with food and water *ad libitum*. Four- to 5-week-old mice received subcutaneous injection of 5×10^6 MKN45 or EBC-1 cells in 200 μL of PBS or 5×10^6 KP4 cells in 50 μL of 1:1 volume mixture of Hanks' balanced salt solution (Invitrogen) and

Matrigel (BD Biosciences) into the right flank. The U-87MG xenograft studies were conducted by Piedmont using Harlan Laboratories female (Hsd:Athymic Nude-Foxn^{nu}) mice with 1 mm³ tumor fragments implanted subcutaneously into the flank. For all studies, after the tumor xenografts were established, mice with tumors (approximately 150–300 mm³, see Figures) were randomized into groups of ≥ 6 mice. Groups were treated with vehicle, TAK-701 alone, TKI alone, or combination of the two drugs. TAK-701 was diluted in saline just before injection and administered intravenously once or twice a week. TKIs were diluted in a 30% captisol-citrate buffer for administration by oral gavage. Administration volume was 5 to 10 mL/kg.

Tumor volume and endpoints

Tumor sizes were measured twice per week starting one day before the first day of treatment. Tumor weights were calculated using the equation $(L \times W^2)/2$, where L and W refer to the larger and smaller dimensions collected at each measurement, respectively. Antitumor efficacy was expressed as mean relative growth of treated versus control tumors (%T/C) using the formula: $[(T-T_0)/(C-C_0)] \times 100$, in which C and T are mean control and drug-treated tumor volume, and C_0 and T_0 are initial tumor volumes, respectively. Regression percentage was calculated using the formula: $[1 - (T/T_0)] \times 100$, in which T and T_0 are treated and initial tumor volume, respectively.

Statistical analysis

Statistical differences between treatment groups over the treatment period (T-T₀) were analyzed by one-tailed one-way ANOVA, Dunnett test. The Wilcoxon test was used to evaluate the effect of combining TAK-701 and Compound 1, comparing each single-agent group to the combination group. Statistical analyses were carried out with the SAS nonclinical package for Windows (version 5.0; SAS Institute, Inc.). For the U-87MG time to endpoint (TTE) studies, a two-tailed Log-rank (Mantel-Cox) test was used to analyze the significance of the differences between treated and vehicle control groups (Prism version 4, GraphPad Software).

Results

Discovery of selective MET inhibitors with slow off rate

The compound shown in Fig. 1 is derived from the imidazopyridazine chemical series, which is a novel hinge-binder

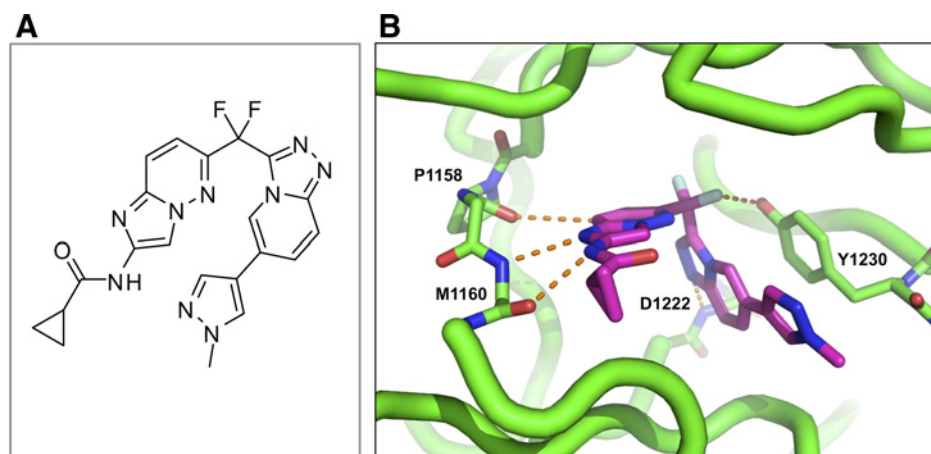
class of MET inhibitors described in WO2010/019899A1. A 2.0 angstrom x-ray diffraction crystal structure of MET in complex with Compound 1 shows the kinase in the DFG-in conformation with the triazolopyridine ring forming a hydrogen bond with the backbone of D1222 and a ring stacking interaction with Y1230. One of the fluoro atoms of the inhibitor linker region also makes a weak interaction with Y1230. Two nitrogen atoms of the imidazopyridazine engage the backbone of hinge residue M1160 via hydrogen bonds. In addition, an aryl CH of the imidazopyridazine forms a pseudo hydrogen bond to the carbonyl of hinge residue P1158. Unique to Compound 1 is a di-fluoromethyl linker that is not present in Compound 2, Compound 3, or other reported selective MET inhibitors (Supplementary Fig. S1). The di-fluoro moiety, in addition to making direct interactions with the protein, also induces subtle electrostatic and conformational effects, which likely influence potency, selectivity, and off-rate.

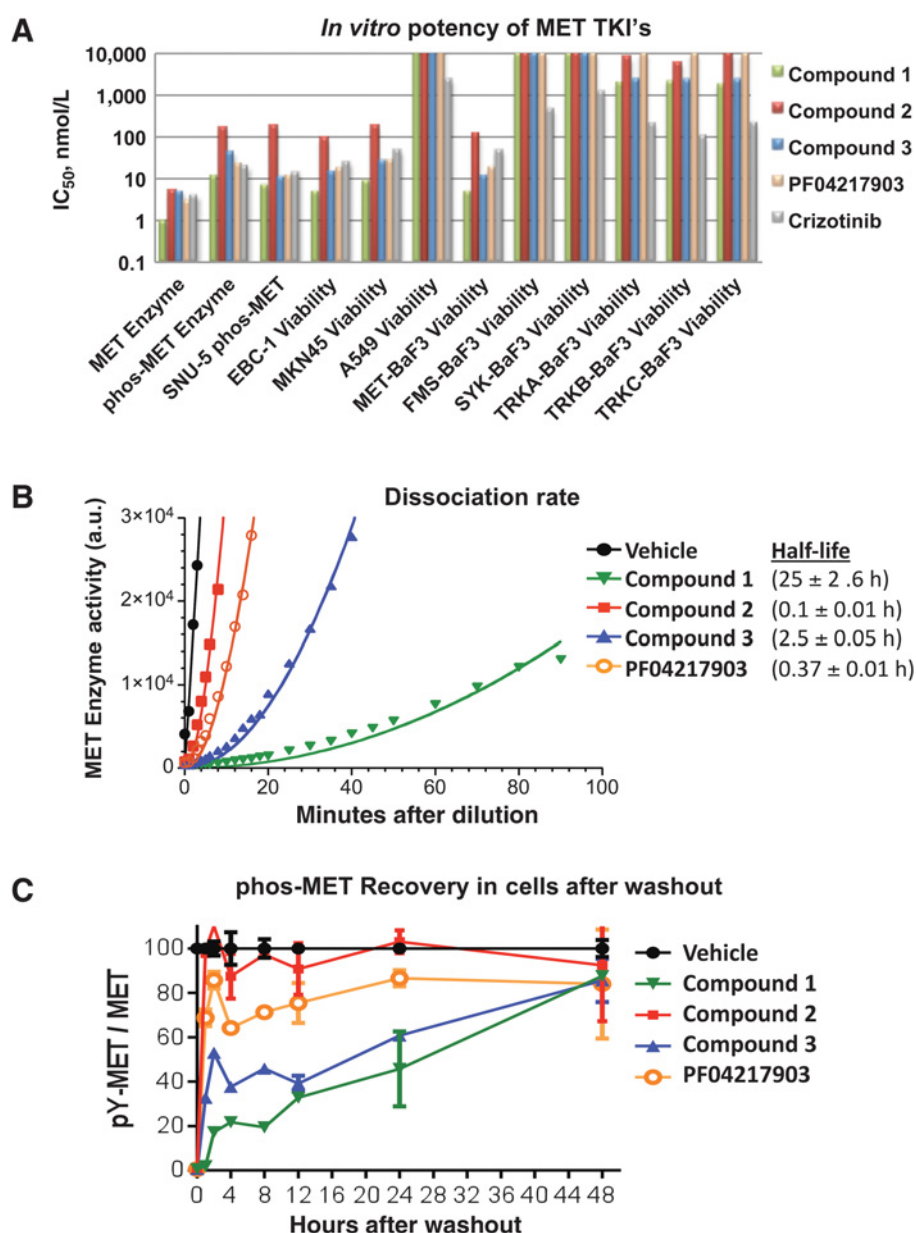
Compound 1 potently inhibits both unphosphorylated and phosphorylated MET enzymes with IC₅₀ < 1 and 12 nmol/L, respectively (Fig. 2A; Supplementary Table S1). A selective MET compound, PF04217903, was used as a reference, and it also exhibited comparable activity. Compound 1 maintained potency (IC₅₀ < 1–57 nmol/L) for the following MET mutants: V1110I, H1112Y, L1195V, Y1235D, D1228H, and M1250T (Supplementary Table S2). Moderate potency was also observed for Y1230 mutations (IC₅₀, 25–280 nmol/L). Interestingly, other selective MET inhibitors do not maintain activity against MET when Y1230 or D1228 is mutated (29, 30).

We evaluated the apparent residence time of inhibition of WT MET by diluting or washing out inhibitor and evaluating the rate of return of enzyme activity *in vitro* with recombinant enzyme or in MKN45 cells (Fig. 2B and C). Compound 1 had the slowest recovery time with half-life in excess of 20 hours, indicating it has a much slower dissociation rate from WT MET than other selective MET inhibitors, including other imidazopyridazines and PF04217903 (Fig. 2B). Thus, Compound 1 is a tight-binding inhibitor of MET with slow dissociation kinetics. The durability of compound activity for inhibiting MET phosphorylation in cells after removing compound was consistent with the enzyme results. The effects of Compound 2 and PF04217903 were reversed in the least time, whereas the effects of Compound 1 and Compound 3 were longer lasting, with approximately 40% to 50%

Figure 1.

Chemical structure and binding mode of Compound 1 to MET. **A**, Compound 1, derived from the imidazopyridazine scaffold, represents a novel MET kinase hinge-binder. It contains a linker region with 2-fluoro atoms and a triazolopyridine ring, which stacks with and orients Y1230 in the active site (**B**), creating a co-complex conformation that is similar to other exquisitely selective MET kinase inhibitors (see Supplementary Fig. S1).



**Figure 2.**

Activity of MET TKIs in enzyme and cellular assessments. **A**, Imidazopyridazine series Compound 1, 2, and 3 were evaluated versus two known MET TKIs, PF04217903 and crizotinib. Enzyme assays were performed with (pY-MET) and without MET preactivation. Cellular assays included mechanism-based (pY1349-MET), end point biology (viability), and selectivity for MET (ATP levels in BaF3 cells expressing the indicated kinase). See Supplementary Table S1 for IC_{50} values. Rate of compound dissociation was evaluated by measuring recovery of MET activity over time after dilution of MET enzyme assays (**B**) or after wash out of compound from MKN45 cells (**C**). Compound dissociation half-life is indicated in **B**.

suppression of MET phosphorylation remaining at 24 hours after washout (Fig. 2C).

The inhibitory activity of the imidazopyridazines was evaluated against a wide range of protein kinases. A total of 130 kinases were examined, and of the three imidazopyridazines, Compound 1 showed the greatest selectivity with at least 50-fold greater activity against MET for >97% of the kinases tested (Supplementary Table S2). The four kinases that were inhibited at high concentrations of Compound 1 (Fms, TrkA, TrkB, and TrkC) were also reported to be inhibited by crizotinib (an inhibitor of ALK/MET), thus we performed further evaluations of kinase selectivity in cells (Fig. 2A; Supplementary Table S1). Compound 1 was at least 350-fold selective for MET in cells versus Trks and Fms, whereas crizotinib appeared less selective and PF04217903 was more selective (Fig. 2A; Supplementary Table S1, BaF3 cell lines).

Inhibition of cellular MET kinase activity was further assessed by measuring MET Y1349 phosphorylation, an established proximal target engagement activity biomarker for MET (8). Compounds 1–3 of the imidazopyridazine chemical series inhibited phosphorylation of MET in a dose-dependent manner in three cell lines overexpressing MET (SNU-5, EBC-1, and MKN45). Average cellular IC_{50} across the three cell lines for Compound 1 was 7 ± 2 nmol/L. Similar potency was observed for Compound 3 and the two reference compounds. However, Compound 2 was about 10-fold less potent (Fig. 2A; Supplementary Table S1).

The effect of the TKIs on cell viability was determined in a panel of three cell lines, the MET-dependent cell lines EBC-1 and MKN45, as well as one cell line not dependent on MET for survival, A549. For Compound 1, viability dose-response curves exhibited complete loss of viability at the E_{max} and the IC_{50} values

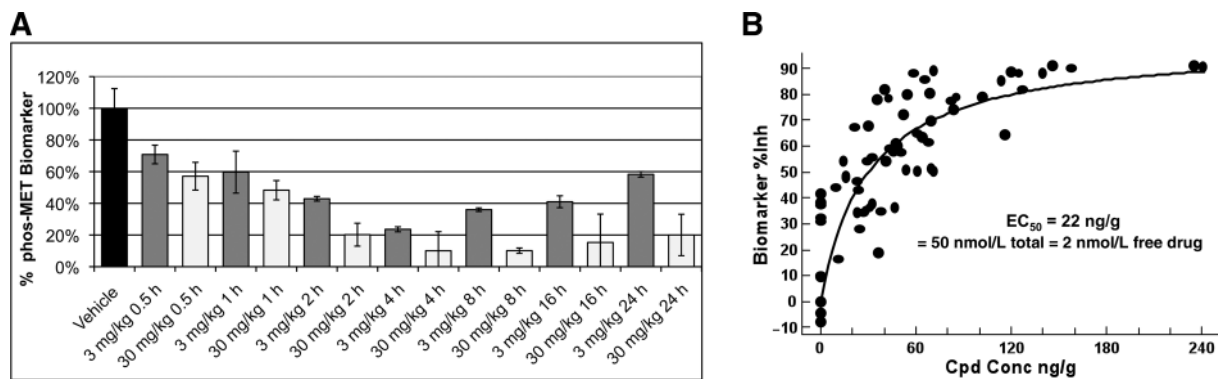


Figure 3.

PD of MET TKI Compound 1 in MKN45 xenografts. **A**, Levels of pY1349 MET were determined in MKN45 tumors harvested at various time points after mice received a single dose of Compound 1. Each bar represents the mean \pm SD of 3 tumor samples tested in duplicate ($n = 6$ technical replicates). **B**, Using individual mouse data, the tumor PK/PD relationship was curve fit using E_{\max} model (Percent inhibition = $[E_{\max} \times (x^n)] / [(x^n) + (EC_{50}^n)]$, where x = drug concentration and n = hill slope factor).

were 5 to 10 nmol/L in EBC-1 and MKN45; as expected, no activity was observed in A549 cells (Fig. 2A; Supplementary Table S1). The cell viability assay potencies correlated well with the cellular MET target engagement potencies for the TKIs. Based on the overall *in vitro* pharmacology, Compound 1 was selected for further evaluation *in vivo*.

Pharmacodynamics and antitumor activity of MET TKI, Compound 1

To determine the appropriate dose range of Compound 1 for efficacy studies and to evaluate the inhibition of MET *in vivo*, PK/pharmacodynamic (PD) analysis was conducted in the MKN45 xenograft model. Suppression of MET phosphorylation in MKN45 tumors over time was determined at two dose levels. Suppression was maximal at 4 hours after dose, and the higher dose demonstrated more durable maximal suppression (Fig. 3A). The PK profile in tumor tissue was also evaluated versus biomarker suppression. The concentration of compound in tumor that produced a 50% reduction of biomarker was 22 ng/g (Fig. 3B). Based on the theory of receptor pharmacology, it is the protein-unbound (free) drug in tissues that interacts with the target to elicit a response (31). The 22 ng/g of Compound 1 is equivalent to 2 nmol/L unbound drug in tumor, when corrected for mouse protein binding to drug and assuming that measured plasma protein binding is equivalent to protein binding in tumor. Based on these data, antitumor therapeutic doses were selected for the evaluation of whether tumor growth inhibition is observed with partial, intermittent suppression of MET versus greater than 90% sustained suppression. As such, daily doses were chosen ranging from 3 mg/kg for intermittent target coverage and twice-daily doses of 30 and 60 mg/kg for maximal target inhibition.

The *in vivo* antitumor efficacy of Compound 1 was evaluated in two MET-dependent xenograft models, MKN45 human gastric adenocarcinoma and EBC-1 human lung squamous cell carcinoma (Fig. 4). Tumor growth was significantly inhibited by Compound 1 in these *in vivo* efficacy models in a dose-dependent manner. A partial tumor growth-inhibitory activity was observed at 2 to 3 mg/kg/d, and stasis of tumor growth was observed at 20 to 30 mg/kg/d. Partial regressions were observed at higher doses or with twice-daily dosing of 30 mg/kg. The

compound was well tolerated at all dose levels with no body weight loss observed. Taken together with the PK/PD analysis, stasis correlates with a high, sustained suppression of MET. Complete regression and tumor-free survival may require complete suppression of phosphorylated MET or combination therapy to dampen other drivers of *in vivo* tumor growth.

Antitumor activity of MET TKI, Compound 1, in combination with HGF antibody

To investigate if dual targeting of MET activation could enhance the efficacy of an MET TKI, we pursued combination with TAK-701, also known as HUL2G7, an antibody that neutralizes HGF. This antibody blocks the binding of HGF to MET, inhibits *in vitro* biological activities of HGF, and causes tumor growth inhibition in HGF-dependent xenografts (32). Combination therapy was evaluated in two HGF/MET-autocrine xenograft models, the pancreatic K-Ras mutant KP4 model and the glioblastoma PTEN mutant U-87MG model (Fig. 5; Supplementary Fig. S2). Both cell lines secrete HGF, express MET, and are sensitive to inhibitors of HGF/MET (30, 33, 34). Twice-weekly *i.v.* administration of 10 mg/kg TAK-701 significantly inhibited KP4 tumor growth (T/C = 57%, $P < 0.025$). Likewise, daily oral (PO) administration of 3 mg/kg Compound 1 significantly inhibited KP4 tumor growth (T/C = 55%, $P < 0.025$). The combination of TAK-701 and Compound 1 resulted in the additive antitumor effect (T/C = 9%, $P < 0.05$). In the U-87MG model, Compound 1 was given at daily doses of 10, 30, and 100 mg/kg, and TAK-701 was given at weekly doses of 1, 3, and 10 mg/kg. The treatment schedule for TAK-701 was reduced to weekly based on the sensitivity of this xenograft model observed previously (32). There was a small but statistically significant tumor growth delay for each monotherapy (TGD of 3–4 days, 26%–32%, $P < 0.05$ at 30–100 mg/kg Compound 1 and TGD of 6–7 days, 47%–58%, $P < 0.01$ at 3–10 mg/kg TAK-701). A remarkable antitumor synergy was apparent when the single agents were combined [TGD of 21 days, 172% with 9 partial regressions (PR) and 1 complete regression (CR), Fig. 5B; Supplementary Fig. S2]. There was a dose-responsive trend toward an increase in the number of complete tumor regressions with TAK-701 in combination with Compound 1 compared with tumor growth stasis and no regression in the

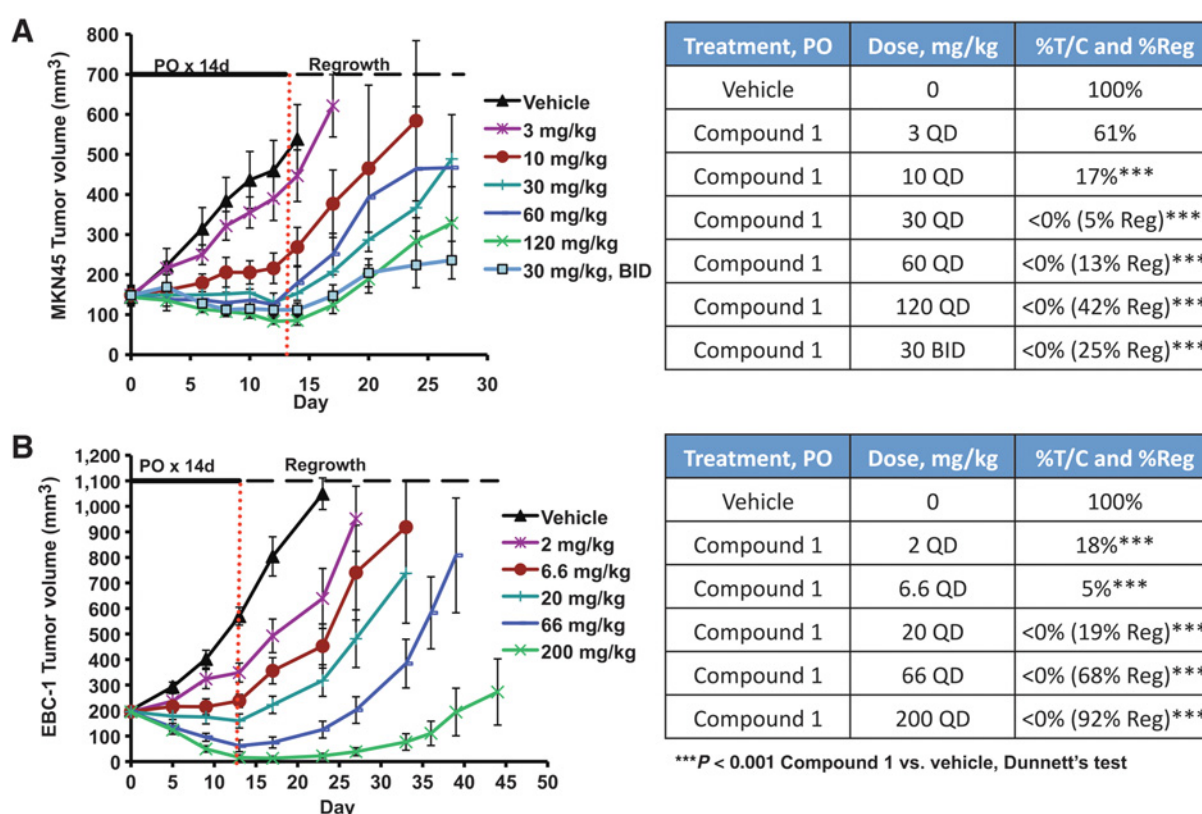


Figure 4.

Antitumor activity of Compound 1 in two MET-dependent xenograft models: MKN45 (**A**) and EBC-1 (**B**). Tumor volumes (mean \pm SEM) were measured over time for each of the indicated groups ($n = 5$ mice per group). Tumor outgrowth was also monitored after treatment cessation. Statistical significance between treatment and vehicle control groups was calculated using one-way ANOVA with Dunnett test (***, $P \leq 0.001$).

single-agent groups. Furthermore, there was a clear a dose-responsive trend toward an increase in TTE survival (Kaplan-Meier plots in Supplementary Fig. S2C). In addition, both compounds were well tolerated in the KP4 and U-87 MG tumor-bearing mice, with no weight loss at any dose levels, alone or in combination.

In a second U-87MG xenograft study, we evaluated if the synergy was specific for Compound 1 or could be observed with other MET TKIs. Two other MET inhibitors in combination with TAK-701 exhibited therapeutic synergy as measured by TGD, TTE, and regressions (Fig. 6A, right; Supplementary Fig. S3). Although the extent of effect for each compound is dependent on the potency (Fig. 2) and the free-drug concentration in the tumor, these results suggest that treatment with the combination of TAK-701 and an MET TKI results in synergy and is superior to single-agent therapy.

To investigate the mechanism by which the MET TKI/HGF antibody produces synergy, the U-87MG tumors were evaluated for inhibition of MET pathway markers on the 5th day of Compound 1 administration. The MET TKI caused a decrease of AKT and ERK phosphorylation at 2 hours, which subsequently recovered by 24 hours. The MET TKI had a greater effect on ERK versus AKT. A single administration of TAK-701 caused partial suppression of ERK and did not alter AKT phosphorylation. The combination therapy produced robust effects on ERK, AKT, and 4E-BP1 at 2 hours; however, while the effect on

4E-BP1 was maintained through 24 hours, the effects on ERK and AKT were not completely maintained (Fig. 6B). Interestingly, each monotherapy did not affect 4E-BP1. Other MET pathway proteins were evaluated to gain insight into the signaling pattern alterations caused by the combination therapy (Supplementary Fig. S4). Tumor samples were also evaluated using the MET immunoassay for assessment of phosphorylated MET and total MET (Fig. 6A, left). The MET TKIs caused an 80% to 90% suppression of phosphorylated MET at 2 hours after dose. By 24 hours, the suppressive effect decreased to 30% to 60%, whereas TAK-701 maintained a partial suppression of 50% to 60% through 24 hours. Combination therapy clearly enhanced the decrease in phosphorylated MET; however, it was not completely suppressed as 10% to 20% remained at 24 hours after dose (Fig. 6A). A striking finding from this analysis was the effect of the therapies on total MET. The monotherapies appeared to increase total MET, whereas the combination therapies decreased total MET. The decrease in MET at 24 hours appears to correlate with the level of efficacy for the combination therapies. In summary, the biomarker evaluation suggests that the synergy may be a result of effects on 4E-BP1 and MET.

Discussion

In this study, we provide the *in vitro* and *in vivo* characterization of the preclinical activity of a selective, oral MET TKI and

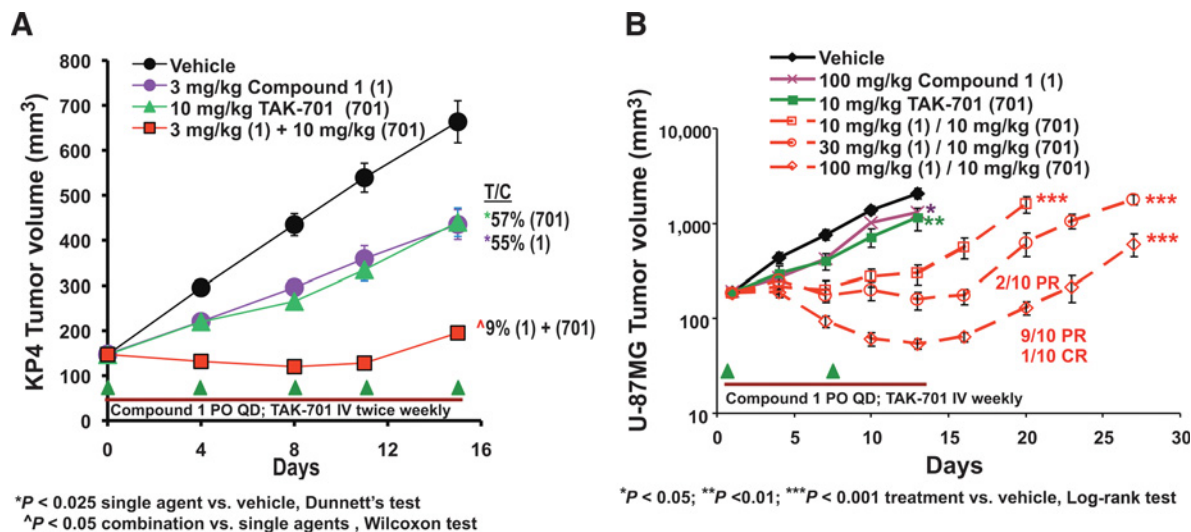


Figure 5.

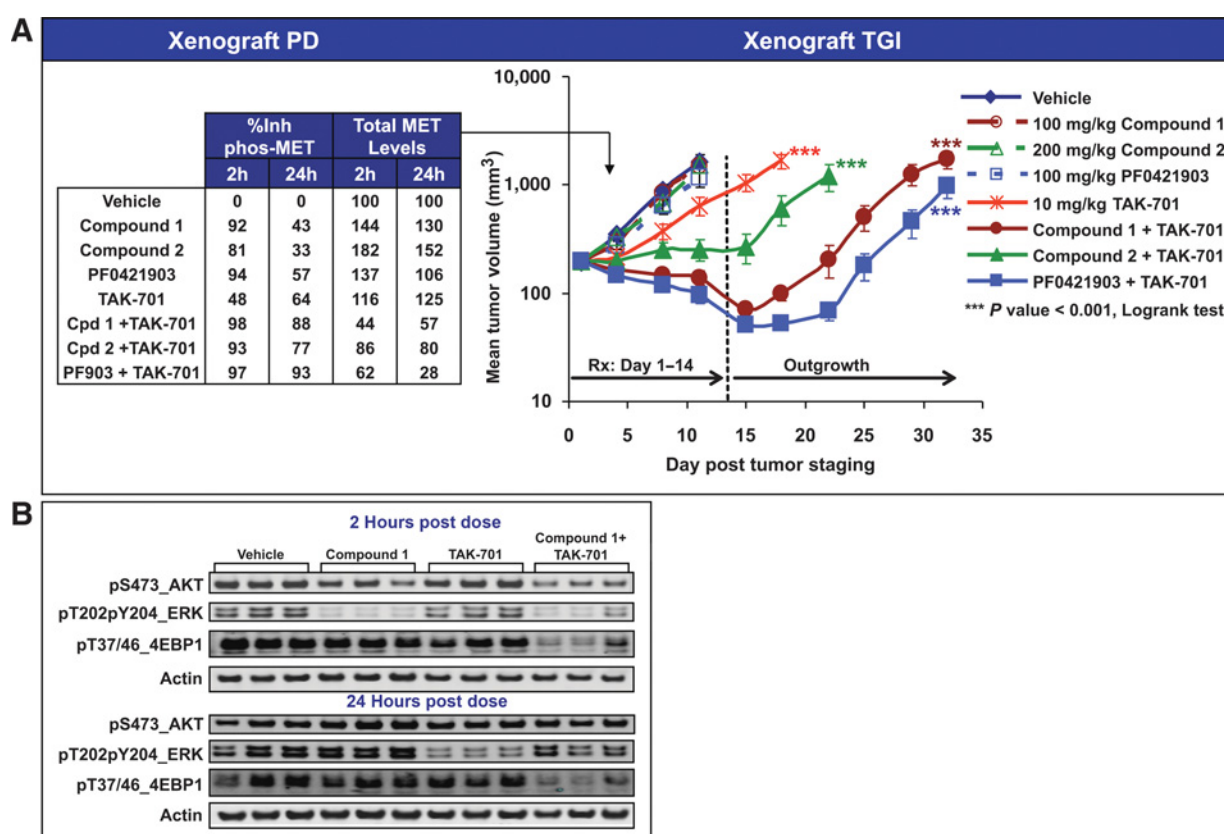
Compound 1 enhances the efficacy of an HGF-neutralizing antibody. Mice with KP4 pancreatic xenografts (**A**) or U-87MG glioblastoma xenografts (**B**) were treated with the indicated regimens ($n = 6$ or 10 mice per group, respectively, for KP4 or U-87MG xenografts). Tumor volumes (mean \pm SEM) were measured over time. Significance of single-agent treatments versus vehicle control KP4 tumors was determined using one-way ANOVA with Dunnett test (*, $P < 0.025$), and significance of single agents versus combination was determined using the Wilcoxon test (*, $P < 0.05$). Tumor outgrowth after treatment cessation was monitored in the U-87MG model, and the Log-rank test was used to determine statistical significance in TTE between treatment groups and vehicle control group (*, $P < 0.05$; **, $P < 0.01$; and ***, $P < 0.001$). See Supplementary Fig. S2 for additional results.

its synergistic antitumor effects when combined with an anti-HGF antibody. Compound 1 potently inhibits MET and MET biological activity in several *in vitro* assessments, including MET enzyme assays and cellular assays, evaluating phosphorylation of MET and tumor cell viability. Compound 1 exhibited a high degree of selectivity versus other kinases in enzyme and cellular assays. The distinctive DFG-in binding mode, engaging Y1230 in the active site, most likely contributes to the selectivity, similar to other selective type I MET inhibitors (35). Compound 1 also maintains significant activity against described mutations of MET, including V1110I, H1112Y, L1195V, Y1235D, D1228H, and M1250T, and exhibits moderate activity against Y1230H, Y1230C, and Y1230D, demonstrating broad spectrum activity against MET mutants. Furthermore, the effect of Compound 1 is durable in enzyme dissociation assays and cellular assays after removal of compound. The inhibitory effect of Compound 1, provided by the distinct di-fluoro binding mode filling space in the ATP-binding pocket, outlasted other selective MET TKIs, thus making it uniquely durable among the compounds tested. Importantly, and as expected, oral administration of Compound 1 to tumor-bearing mice blocked MET-dependent tumor cell growth *in vivo* through decreasing phosphorylated MET and downstream signaling in four xenograft models, including MET-dependent models and autocrine HGF/MET models. Evaluation of the PK/PD/E relationship indicated that sustained >80% to 90% inhibition of MET phosphorylation correlated with stasis of tumor proliferation. To sum up, Compound 1, a unique, potent, selective, orally available MET TKI with slow dissociation kinetics, exhibited the desired *in vivo* PD and antitumor activities to treat MET-dependent cancers.

Intriguingly, Compound 1 in combination with an HGF-neutralizing antibody reduced total MET protein and resulted in enhanced antitumor effect. This biological effect and mechanism

cannot be explained by the slow dissociation kinetics of Compound 1 with MET, since similar effects were observed with MET TKIs that exhibited fast dissociation kinetics. Treatment of cells with MET TKIs is reported to prevent MET endocytosis, leading to an accumulation of MET at the cell surface (36). This effect is consistent with our result showing that MET TKI monotherapy induces an increase in total MET in U-87MG tumors *in vivo*. In addition, stimulation with HGF decreases total MET levels (37), and our results show that blocking HGF increases total MET levels in the U-87MG tumors. It was unexpected that simultaneously blocking MET kinase activity and neutralizing HGF resulted in reduction of total MET (as opposed to a further increase). The sustained decrease in 4E-BP1 phosphorylation induced by the combination therapy suggests that a translational arrest may be involved in the mechanism and increased control of the noncanonical signaling of MET resulting in receptor downregulation with the combination. However, the effect on 4E-BP1 may also be an independent effect, and more investigations are needed to clarify this.

Abrogation of MET phosphorylation is not sustained through 24 hours with single-agent therapy (TKI or anti-HGF), likely because the treatment induces resistance mechanisms and/or MET inhibition is incomplete during the time period between doses. The combination therapy tested in this study targets molecules in the same signaling pathway (HGF ligand and MET RTK) and results in a more sustained MET inhibition and enhanced antitumor response and likely tumor cell killing, as exhibited by the partial tumor regressions. PARP cleavage, an indicator of apoptosis, was observed in the tumors from mice receiving the combination therapy. However, these data were variable between mice, and more investigation is needed to understand the heterogeneity of these apoptotic biomarkers and may explain variability of tumor response.

**Figure 6.**

Combination synergy correlates with sustained suppression of MET phosphorylation, reduction of MET protein levels, and reduction of 4E-BP1 phosphorylation. Mice bearing U-87MG xenografts ($n = 10$ mice per group) were treated with the indicated regimen (**A**, right). MET TKIs were administered daily via oral gavage, and TAK-701 was administered weekly via i.v. route. Tumor volumes (mean \pm SEM) were measured over time. Statistical differences in TTE vs. vehicle group were calculated using the Log-rank test. See Supplementary Fig. S3 for the Kaplan-Meier survival plot. Two separate cohorts of mice were sacrificed for the pathway biomarker analysis, one on day 5 at 2 hours after dose and the other on day 5 at 24 hours after dose ($n = 3$ mice per group for each group: 100 mg/kg Compound 1, 10 mg/kg TAK-701, and 100 mg/kg Compound 1 + 10 mg/kg TAK-701). Phosphorylated MET and total MET were evaluated by immunoassay (**A**, left) and ERK, and PI3K/AKT pathway markers were evaluated by Western blot (**B**). See Supplementary Figures for additional results.

One speculative possibility to explain why the TKI/anti-HGF combination is more sustained and effective than the single-agent therapy is that simultaneously blocking HGF and MET kinase could alter receptor dynamics, stability, shedding, or endocytosis, leading to loss of MET receptor. Another possibility beyond plasma membrane signaling is perturbations in the balance between degradation and recycling of MET in endosomes. Several specific mechanisms have been implicated in regulating MET levels, including protease-mediated MET shedding, Cbl-mediated ubiquitination and degradation of MET, disruption of Hsp90-MET complexes, MET internalization/endocytosis, degradation by lysosomes, and mechanisms that regulate transcription of MET (36, 38–46). In one example, MET endocytic trafficking was shown to be required for the full activation of signals such as Gab1, ERK 1/2, STAT3, and Rac1 (46). Gab1 was also reported to be involved in the pathway downstream of HGF-dependent MET activation in tumor xenografts (27). This pathway was shown to be qualitatively different from the pathway downstream of overexpression-induced MET activation, thus implicating two distinct yet redundant pathways in terms of cell survival. The redundant pathways

include restoration of PI3K signaling through recruitment of the Gab1 adaptor following HGF stabilization of MET homodimers and signal transduction initiated from overexpression-induced homodimers or heterodimers of MET with other receptors, including EGFR family members (27). Although U-87MG tumor xenografts normally utilize autocrine HGF to activate MET and maintain tumor cell survival, monotherapy treatment with TKI or anti-HGF increased total MET levels. This provides the tumor the potential to use that alternate distinct survival pathway initiated from MET homodimers or heterodimers. Our analysis of the signaling pathway in U-87MG xenografts shows that the TKI/anti-HGF combination results not only in reduction of MET but also in EGFR, Src, beta-catenin, and 4E-BP1 (Fig. 6B; Supplementary Fig. S4), suggesting these proteins could be involved in the combination mechanism. For example, it is conceivable that single-agent treatment is inducing MET:EGFR heterodimers and downstream signaling through increasing MET and that the combination prevents this through reduction of MET and 4E-BP1. To further explore the pathway and protein interactions, more investigations are needed, such as RNAi/CRISPER, and may

lead to an understanding of the underlying mechanism along with the discovery of additional combinations that decrease total MET and triggering therapeutic synergy.

The rebound in tumor growth after withdrawal of treatment is typical after a lag period and is attributable to both the duration and effectiveness of the anticancer treatment. Tumor cells may be utilizing multiple growth mechanisms and/or resistance mechanisms to maintain the tumor and heterogeneity of response. The scope of treatment-based resistance mechanisms is not completely known and is part of on-going investigations throughout the research community. Possible mechanisms for the lack of complete response to the combination treatment in this study could include selection for secondary resistance mutations like a point mutation in the activation loop of MET, amplification of KRAS, and "oncogene kinase switch" systems (such as insulin-like growth factor-1 receptor or EGFR) to bypass MET pathways in resistant tumor cells (47).

Because targeting HGF and MET within the same signaling pathway did lead to better efficacy, we have investigated other combination therapies which target two molecules within the MET pathway. Combination of the MET TKI with an MEK inhibitor (TAK-733; ref. 48) or with a PI3K inhibitor (pictilisib) did produce additive or synergistic effects on cell viability (Supplementary Fig. S5). These additional MET TKI combination approaches have potential therapeutic application for cancers that utilize HGF/MET as a primary driver or co-driver of growth and/or metastasis including cancers that have upregulated MET activity as a resistance mechanism to other therapies.

The preclinical antitumor activity of the dual inhibition of MET ligand with TAK-701 and MET tyrosine kinase activity with Compound 1 was explored in experimental *in vivo* tumor models. The combination of inhibitors produces a unique mechanistic interaction. This interaction increases inhibition of MET and 4E-BP1, decreases total MET, and leads to additive or synergistic antitumor activity as well as prolonged inhibition of tumor regrowth after cessation of treatment compared to either single agent alone. Combined treatment with Compound 1 and TAK-701 is superior to single-agent therapy as the unique mechanism induced by the combination therapy leads to additive or synergistic inhibition of tumor growth. Preclinical *in vitro* and *in vivo* antitumor data now demonstrate a compelling biological rationale to use an MET TKI in combination with an antibody to HGF in clinical trials for patients with advanced malignancies. In

summary, the present study illustrates the potential of targeting MET-dependent tumors with a novel MET TKI/Anti-HGF combination and provides an opportunity to expand the value of each single agent by increasing the number of cancer patients who respond to therapy.

Disclosure of Potential Conflicts of Interest

P.J. Farrell is an associate director at Takeda. No potential conflicts of interest were disclosed by the other authors.

Authors' Contributions

Conception and design: P.J. Farrell, S. Chu, R. de Jong, P. Vincent

Development of methodology: P.J. Farrell, D. Balakrishna, R. Kamran, S. Chu, P. Vincent

Acquisition of data (provided animals, acquired and managed patients, provided facilities, etc.): P.J. Farrell, J. Matuszkiewicz, S. Pandya, M.S. Hixon, A. Hori, A. Mizutani, H. Iwata, P. Vincent

Analysis and interpretation of data (e.g., statistical analysis, biostatistics, computational analysis): P.J. Farrell, J. Matuszkiewicz, S. Pandya, M.S. Hixon, S. Chu, J.D. Lawson, K. Okada, A. Hori, A. Mizutani, H. Iwata, P. Vincent

Writing, review, and/or revision of the manuscript: P.J. Farrell, J. Matuszkiewicz, M.S. Hixon, S. Chu, J.D. Lawson, A. Hori, R. de Jong, B. Hibner, P. Vincent

Administrative, technical, or material support (i.e., reporting or organizing data, constructing databases): P.J. Farrell, J.D. Lawson, B. Hibner

Study supervision: P.J. Farrell, S. Chu, P. Vincent

Acknowledgments

The authors thank Galaxy Biotech, LLC for the HGF antibody; Piedmont for conducting the U-87MG xenograft studies; Jasmine Nguyen for the purified MET protein; Shawn O'Connell, Robyn Fabrey, Andrew Stanton, and Jason Kahana for help with the xenograft studies; Aixia Sun for PK analysis; Isaac Hoffman for help with crystal structures; Petro Halkowycz for contributing to enzyme assessments; Mike Wallace and Phil Erikson for chemical design; and Jeffery Stafford for strategy discussions. The authors thank the TCAL MET project team for their technical and scientific contributions.

Grant Support

This work was supported by Takeda Pharmaceuticals.

The costs of publication of this article were defrayed in part by the payment of page charges. This article must therefore be hereby marked *advertisement* in accordance with 18 U.S.C. Section 1734 solely to indicate this fact.

Received November 15, 2016; revised December 13, 2016; accepted March 15, 2017; published OnlineFirst March 24, 2017.

References

- Fajardo-Puerta AB, Mato Prado M, Frampton AE, Jiao LR. Gene of the month: HGF. *J Clin Pathol* 2016;69:575–9.
- Garajova I, Giovannetti E, Biasco G, Peters GJ. c-Met as a target for personalized therapy. *Transl Oncogenomics* 2015;7:13–31.
- Skead G, Govender D. Gene of the month: MET. *J Clin Pathol* 2015;68:405–9.
- Trusolino L, Bertotti A, Comoglio PM. MET signalling: Principles and functions in development, organ regeneration and cancer. *Nat Rev Mol Cell Biol* 2010;11:834–48.
- Birchmeier C, Birchmeier W, Gherardi E, Vande Woude GF. Met, metastasis, motility and more. *Nat Rev Mol Cell Biol* 2003;4:915–25.
- Boccaccio C, Comoglio PM. MET, a driver of invasive growth and cancer clonal evolution under therapeutic pressure. *Curr Opin Cell Biol* 2014;31:98–105.
- Smyth EC, Sclafani F, Cunningham D. Emerging molecular targets in oncology: Clinical potential of MET/hepatocyte growth-factor inhibitors. *OncoTargets Ther* 2014;7:1001–14.
- Zhang Y, Du Z, Zhang M. Biomarker development in MET-targeted therapy. *Oncotarget* 2016;7:37370–89.
- Van Der Steen N, Pauwels P, Gil-Bazo I, Castanon E, Raez L, Cappuzzo F, Rolfo C. cMET in NSCLC: Can we cut off the head of the hydra? from the pathway to the resistance. *Cancers* 2015;7:556–73.
- Engelman JA, Zejnullahu K, Mitsudomi T, Song Y, Hyland C, Park JO, et al. MET amplification leads to gefitinib resistance in lung cancer by activating ERBB3 signaling. *Science* 2007;316:1039–43.
- Hage C, Rausch V, Giese N, Giese T, Schonsiegel F, Labsch S, et al. The novel c-Met inhibitor cabozantinib overcomes gemcitabine resistance and stem cell signaling in pancreatic cancer. *Cell Death Dis* 2013;4:e627.
- Ishikawa D, Takeuchi S, Nakagawa T, Sano T, Nakade J, Nanjo S, et al. mTOR inhibitors control the growth of EGFR mutant lung cancer even after acquiring resistance by HGF. *PloS One* 2013;8:e62104.
- Jahangiri A, De Lay M, Miller LM, Carbonell WS, Hu YL, Lu K, et al. Gene expression profile identifies tyrosine kinase c-Met as a targetable

- mediator of antiangiogenic therapy resistance. *Clin Cancer Res* 2013;19:1773–83.
14. Minuti G, Cappuzzo F, Duchnowska R, Jassem J, Fabi A, O'Brien T, et al. Increased MET and HGF gene copy numbers are associated with trastuzumab failure in HER2-positive metastatic breast cancer. *Br J Cancer* 2012;107:793–9.
 15. Nakagawa T, Takeuchi S, Yamada T, Nanjo S, Ishikawa D, Sano T, et al. Combined therapy with mutant-selective EGFR inhibitor and Met kinase inhibitor for overcoming erlotinib resistance in EGFR-mutant lung cancer. *Mol Cancer Ther* 2012;11:2149–57.
 16. Saito S, Morishima K, Ui T, Hoshino H, Matsubara D, Ishikawa S, et al. The role of HGF/MET and FGF/FGFR in fibroblast-derived growth stimulation and lapatinib-resistance of esophageal squamous cell carcinoma. *BMC Cancer* 2015;15:82.
 17. Shojaei F, Lee JH, Simmons BH, Wong A, Esparza CO, Plumlee PA, et al. HGF/c-Met acts as an alternative angiogenic pathway in sunitinib-resistant tumors. *Cancer Res* 2010;70:10090–100.
 18. Song N, Liu S, Zhang J, Liu J, Xu L, Liu Y, et al. Cetuximab-induced MET activation acts as a novel resistance mechanism in colon cancer cells. *Int J Mol Sci* 2014;15:5838–51.
 19. Cecchi F, Rabe DC, Bottaro DP. Targeting the HGF/Met signaling pathway in cancer therapy. *Expert Opin Ther Targets* 2012;16:553–72.
 20. Ariyawutyakorn W, Saichamchan S, Varella-Garcia M. Understanding and targeting MET signaling in solid tumors - are we there yet? *J Cancer* 2016;7:633–49.
 21. Qi J, McTigue MA, Rogers A, Lifshits E, Christensen JG, Janne PA, et al. Multiple mutations and bypass mechanisms can contribute to development of acquired resistance to MET inhibitors. *Cancer Res* 2011;71:1081–91.
 22. Cavazzoni A, Alfieri RR, Cretella D, Saccani F, Ampollini L, Galetti M, et al. Combined use of anti-ErbB monoclonal antibodies and erlotinib enhances antibody-dependent cellular cytotoxicity of wild-type erlotinib-sensitive NSCLC cell lines. *Mol Cancer* 2012;11:91.
 23. Pirazzoli V, Ayeni D, Meador CB, Sanganaalli BG, Hyder F, de Stanchina E, et al. Afatinib plus cetuximab delays resistance compared to single-agent erlotinib or afatinib in mouse models of TKI-naïve EGFR L858R-induced lung adenocarcinoma. *Clin Cancer Res* 2016;22:426–35.
 24. Regales L, Gong Y, Shen R, de Stanchina E, Vivanco I, Goel A, et al. Dual targeting of EGFR can overcome a major drug resistance mutation in mouse models of EGFR mutant lung cancer. *J Clin Invest* 2009;119:3000–10.
 25. Yonesaka K, Hirotani K, Kawakami H, Takeda M, Kaneda H, Sakai K, et al. Anti-HER3 monoclonal antibody patritumab sensitizes refractory non-small cell lung cancer to the epidermal growth factor receptor inhibitor erlotinib. *Oncogene* 2016;35:878–86.
 26. Wang M, Zhao J, Zhang LM, Li H, Yu JP, Ren XB, et al. Combined erlotinib and cetuximab overcome the acquired resistance to epidermal growth factor receptors tyrosine kinase inhibitor in non-small-cell lung cancer. *J Cancer Res Clin Oncol* 2012;138:2069–77.
 27. Pennacchietti S, Cazzanti M, Bertotti A, Rideout WM3rd, Han M, Gyuris J, et al. Microenvironment-derived HGF overcomes genetically determined sensitivity to anti-MET drugs. *Cancer Res* 2014;74:6598–609.
 28. Morrison JF, Walsh CT. The behavior and significance of slow-binding enzyme inhibitors. *Adv Enzymol Relat Areas Mol Biol* 1988;61:201–301.
 29. Hughes PE, Rex K, Caenepel S, Yang Y, Zhang Y, Broome MA, et al. In vitro and in vivo activity of AMG 337, a potent and selective MET kinase inhibitor, in MET-dependent cancer models. *Mol Cancer Ther* 2016;15:1568–79.
 30. Zou HY, Li Q, Lee JH, Arango ME, Burgess K, Qiu M, et al. Sensitivity of selected human tumor models to PF-04217903, a novel selective c-Met kinase inhibitor. *Mol Cancer Ther* 2012;11:1036–47.
 31. Smith DA, Di L, Kerns EH. The effect of plasma protein binding on in vivo efficacy: Misconceptions in drug discovery. *Nat Rev Drug Discov* 2010;9:929–39.
 32. Kim KJ, Wang L, Su YC, Gillespie GY, Salhotra A, Lal B, et al. Systemic anti-hepatocyte growth factor monoclonal antibody therapy induces the regression of intracranial glioma xenografts. *Clin Cancer Res* 2006;12:1292–8.
 33. Jin H, Yang R, Zheng Z, Romero M, Ross J, Bou-Reslan H, et al. MetMab, the one-armed 5D5 anti-c-Met antibody, inhibits orthotopic pancreatic tumor growth and improves survival. *Cancer Res* 2008;68:4360–8.
 34. Yan SB, Peek VL, Ajamie R, Buchanan SG, Graff JR, Heidler SA, et al. LY2801653 is an orally bioavailable multi-kinase inhibitor with potent activity against MET, MST1R, and other oncoproteins, and displays anti-tumor activities in mouse xenograft models. *Invest New Drugs* 2013;31:833–44.
 35. Underiner TL, Herbertz T, Miknyoczki SJ. Discovery of small molecule c-Met inhibitors: Evolution and profiles of clinical candidates. *Anticancer Agents Med Chem* 2010;10:7–27.
 36. Pupo E, Ducano N, Lupo B, Vigna E, Avanzato D, Perera T, et al. Rebound effects caused by withdrawal of MET kinase inhibitor are quenched by a MET therapeutic antibody. *Cancer Res* 2016;76:5019–29.
 37. Hammond DE, Carter S, Clague MJ. Met receptor dynamics and signalling. *Curr Top Microbiol Immunol* 2004;286:21–44.
 38. Bachleitner-Hofmann T, Sun MY, Chen CT, Liska D, Zeng Z, Viale A, et al. Antitumor activity of SNX-2112, a synthetic heat shock protein-90 inhibitor, in MET-amplified tumor cells with or without resistance to selective MET inhibition. *Clin Cancer Res* 2011;17:122–33.
 39. Petrelli A, Gilestro GF, Lanzardo S, Comoglio PM, Migone N, Giordano S. The endophilin-CIN85-Cbl complex mediates ligand-dependent down-regulation of c-Met. *Nature* 2002;416:187–90.
 40. Carter S, Urbe S, Clague MJ. The met receptor degradation pathway: Requirement for Lys48-linked polyubiquitin independent of proteasome activity. *J Biol Chem* 2004;279:52835–9.
 41. Hammond DE, Urbe S, Vande Woude GF, Clague MJ. Down-regulation of MET, the receptor for hepatocyte growth factor. *Oncogene* 2001;20:2761–70.
 42. Prat M, Crepaldi T, Gandino L, Giordano S, Longati P, Comoglio P. C-terminal truncated forms of Met, the hepatocyte growth factor receptor. *Mol Cell Biol* 1991;11:5954–62.
 43. Kubic JD, Little EC, Lui JW, Iizuka T, Lang D. PAX3 and ETS1 synergistically activate MET expression in melanoma cells. *Oncogene* 2015;34:4964–74.
 44. Ogunwobi OO, Puszyk W, Dong HJ, Liu C. Epigenetic upregulation of HGF and c-Met drives metastasis in hepatocellular carcinoma. *PLoS One* 2013;8:e63765.
 45. Ide T, Kitajima Y, Miyoshi A, Ohtsuka T, Mitsuno M, Ohtaka K, et al. Tumor-stromal cell interaction under hypoxia increases the invasiveness of pancreatic cancer cells through the hepatocyte growth factor/c-Met pathway. *Int J Cancer* 2006;119:2750–9.
 46. Barrow-McGee R, Kermorgant S. Met endosomal signalling: In the right place, at the right time. *Int J Biochem Cell Biol* 2014;49:69–74.
 47. Sierra JR, Tsao M-S. c-MET as a potential therapeutic target and biomarker in cancer. *Ther Adv Med Oncol* 2011;3:S21–S35.
 48. Dong Q, Dougan DR, Gong X, Halkowycz P, Jin B, Kanouni T, et al. Discovery of TAK-733, a potent and selective MEK allosteric site inhibitor for the treatment of cancer. *Bioorg Med Chem Lett* 2011;21:1315–9.